Low-bias current 10 Gbit/s direct modulation of GaInAsP/InP membrane DFB laser on silicon

Daisuke Inoue,[1,*] **Takuo Hiratani,**[1] **Kai Fukuda,**[1] **Takahiro Tomiyasu,**[1] **Tomohiro Amemiya,**[1,2] **Nobuhiko Nishiyama,**[1,2] **and Shigehisa Arai**[1,2]

[1]*Department of Electrical and Electronic Engineering, Tokyo Institute of Technology, 2-12-1-S9-5 O-okayama, Meguro-ku, Tokyo 152-8552, Japan*
[2]*Institute of Innovative Research (IIR), Tokyo Institute of Technology, 2-12-1-S9-5 O-okayama, Meguro-ku, Tokyo 152-8552, Japan*
[*]inoue.d.ac@m.titech.ac.jp

Abstract: Low-power consumption directly-modulated lasers are a key device for on-chip optical interconnection. We fabricated a GaInAsP/InP membrane DFB laser that exhibited a low-threshold current of 0.21 mA and single-mode operation with a sub-mode suppression ratio of 47 dB at a bias current of 2 mA. A high modulation efficiency of 11 GHz/mA$^{1/2}$ was obtained. A 10 Gbit/s direct modulation using a non-return-to-zero 2^{31}-1 pseudo-random bit sequence signal was performed with a bias current of 1 mA, which is the lowest bias current ever reported for direct modulation of a DFB laser. A bit-error rate of 10^{-9} was successfully achieved.

References and links

1. M. A. Taubenblatt, "Optical interconnects for high-performance computing," J. Lightwave Technol. **30**(4), 448–457 (2012).
2. D. A. B. Miller, "Rationale and challenges for optical interconnects to electronic chips," Proc. IEEE **88**(6), 728–749 (2000).
3. M. Haurylau, G. Chen, H. Chen, J. Zhang, N. A. Nelson, D. H. Albonesi, E. G. Friedman, and P. M. Fauchet, "On-chip optical interconnect roadmap: challenges and critical directions," IEEE J. Sel. Top. Quantum Electron. **12**(6), 1699–1705 (2006).
4. N. Ophir, K. Padmaraju, A. Biberman, L. Chen, K. Preston, M. Lipson, and K. Bergman, "First demonstration of error-free operation of a full silicon on-chip photonic link," in *Optical Fiber Communication Conference*, 2011 OSA Technical Digest Series (Optical Society of America, 2011), paper OWZ3.
5. X. Xiao, H. Xu, X. Li, Z. Li, Y. Yu, and J. Yu, "High-speed on-chip photonic link based on ultralow-power microring modulator," in *Optical Fiber Communication Conference*, 2014 OSA Technical Digest Series (Optical Society of America, 2014), paper Tu2E.
6. D. A. B. Miller, "Device requirements for optical interconnects to silicon chips," Proc. IEEE **97**(7), 1166–1185 (2009).
7. W. Hofmann, P. Moser, and D. Bimberg, "Energy-efficient VCSELs for interconnects," IEEE Photonics J. **4**(2), 652–656 (2012).
8. J. Van Campenhout, P. Rojo Romeo, P. Regreny, C. Seassal, D. Van Thourhout, S. Verstuyft, L. Di Cioccio, J.-M. Fedeli, C. Lagahe, and R. Baets, "Electrically pumped InP-based microdisk lasers integrated with a nanophotonic silicon-on-insulator waveguide circuit," Opt. Express **15**(11), 6744–6749 (2007).
9. S. Matsuo, T. Sato, K. Takeda, A. Shinya, K. Nozaki, H. Taniyama, M. Notomi, K. Hasebe, and T. Kakitsuka, "Ultralow operating energy electrically driven photonic crystal lasers," IEEE J. Sel. Top. Quantum Electron. **19**(4), 4900311 (2013).
10. M. H. MacDougal, G. M. Yang, and P. D. Dapkus, "Ultralow threshold current vertical-cavity surface-emitting lasers obtained with selective oxidation," Electron. Lett. **31**(11), 886–888 (1995).
11. K. Takeda, T. Sato, A. Shinya, K. Nozaki, W. Kobayashi, H. Taniyama, M. Notomi, K. Hasebe, T. Kakitsuka, and S. Matsuo, "Few-fJ/bit data transmissions using directly modulated lambda-scale embedded active region photonic-crystal lasers," Nat. Photonics **7**(7), 569–575 (2013).

12. P. Moser, J. A. Lott, P. Wolf, G. Larisch, H. Li, N. N. Ledentsov, and D. Bimberg, "56 fJ dissipated energy per bit of oxide-confined 850 nm VCSELs operating at 25 Gbit/s," Electron. Lett. **48**(20), 1292–1294 (2012).

13. T. Okamoto, N. Nunoya, Y. Onodera, S. Tamura, and S. Arai, "Continuous wave operation of optically pumped membrane DFB laser," Electron. Lett. **37**(24), 1455–1457 (2001).

14. S. Arai, N. Nishiyama, T. Maruyama, and T. Okumura, "GaInAsP/InP membrane lasers for optical interconnects," IEEE J. Sel. Top. Quantum Electron. **17**(5), 1381–1389 (2011).

15. R. Nagarajan, M. Kato, J. Pleumeekers, P. Evans, S. Corzine, S. Hurtt, A. Dentai, S. Murthy, M. Missey, R. Muthiah, R. A. Salvatore, C. Joyner, R. Schneider, M. Ziari, F. Kish, and D. Welch, "InP photonic integrated circuits," IEEE J. Sel. Top. Quantum Electron. **16**(5), 1113–1125 (2010).

16. W. Kobayashi, T. Ito, T. Yamanaka, T. Fujisawa, Y. Shibata, T. Kurosaki, M. Kohtoku, T. Tadokoro, and H. Sanjoh, "50-Gb/s direct modulation of 1.3-μm InGaAlAs-based DFB laser with ridge waveguide structure," IEEE J. Sel. Top. Quantum Electron. **19**(4), 1500908 (2013).

17. T. Okamoto, N. Nunoya, Y. Onodera, T. Yamazaki, S. Tamura, and S. Arai, "Optically pumped membrane BH-DFB lasers for low-threshold and single-mode operation," IEEE J. Sel. Top. Quantum Electron. **9**(5), 1361–1366 (2003).

18. T. Maruyama, T. Okumura, S. Sakamoto, K. Miura, Y. Nishimoto, and S. Arai, "GaInAsP/InP membrane BH-DFB lasers directly bonded on SOI substrate," Opt. Express **14**(18), 8184–8188 (2006).

19. S. Sakamoto, H. Naitoh, M. Ohtake, Y. Nishimoto, S. Tamura, T. Maruyama, N. Nishiyama, and S. Arai, "Strongly index-coupled membrane BH-DFB lasers with surface corrugation grating," IEEE J. Sel. Top. Quantum Electron. **13**(5), 1135–1141 (2007).

20. K. Oe, Y. Noguchi, and C. Caneau, "GaInAsP lateral current injection lasers on semi-insulating substrates," IEEE Photonics Technol. Lett. **6**(4), 479–481 (1994).

21. T. Okumura, M. Kurokawa, M. Shirao, D. Kondo, H. Ito, N. Nishiyama, T. Maruyama, and S. Arai, "Lateral current injection GaInAsP/InP laser on semi-insulating substrate for membrane-based photonic circuits," Opt. Express **17**(15), 12564–12570 (2009).

22. T. Shindo, T. Okumura, H. Ito, T. Koguchi, D. Takahashi, Y. Atsumi, J. Kang, R. Osabe, T. Amemiya, N. Nishiyama, and S. Arai, "GaInAsP/InP lateral-current-injection distributed feedback laser with a-Si surface grating," Opt. Express **19**(3), 1884–1891 (2011).

23. D. Inoue, J. Lee, K. Doi, T. Hiratani, Y. Atsuji, T. Amemiya, N. Nishiyama, and S. Arai, "Room-temperature continuous-wave operation of GaInAsP/InP lateral-current-injection membrane laser bonded on Si substrate," Appl. Phys. Express **7**(7), 072701 (2014).

24. D. Inoue, J. Lee, T. Hiratani, Y. Atsuji, T. Amemiya, N. Nishiyama, and S. Arai, "Sub-milliampere threshold operation of butt-jointed built-in membrane DFB laser bonded on Si substrate," Opt. Express **23**(6), 7771–7778 (2015).

25. D. Inoue, T. Hiratani, K. Fukuda, T. Tomiyasu, T. Amemiya, N. Nishiyama, and S. Arai, "High-modulation efficiency operation of GaInAsP/InP membrane distributed feedback laser on Si substrate," Opt. Express **23**(22), 29024–29031 (2015).

26. D. Inoue, T. Hiratani, Y. Atsuji, T. Tomiyasu, T. Amemiya, N. Nishiyama, and S. Arai, "Monolithic integration of membrane-based butt-jointed built-in DFB lasers and p-i-n photodiodes bonded on Si substrate," IEEE J. Sel. Top. Quantum Electron. **21**(6), 1502907 (2015).

27. T. Hiratani, D. Inoue, T. Tomiyasu, Y. Atsuji, K. Fukuda, T. Amemiya, N. Nishiyama, and S. Arai, "Room-temperature continuous-wave operation of membrane distributed-reflector laser," Appl. Phys. Express **8**(11), 112701 (2015).

28. T. Makino and J. Glinski, "Transfer matrix analysis of the amplified spontaneous emission of DFB semiconductor laser amplifiers," IEEE J. Quantum Electron. **24**(8), 1507–1518 (1988).

29. R. S. Tucker, "High-speed modulation of semiconductor lasers," J. Lightwave Technol. **3**(6), 1180–1192 (1985).

30. R. Olshansky, P. Hill, V. Lanzisera, and W. Powazinik, "Frequency response of 1.3 μm InGaAsP high speed semiconductor lasers," IEEE J. Quantum Electron. **23**(9), 1410–1418 (1987).

31. S. H. Lee, D. Takahashi, T. Shindo, K. Shinno, T. Amemiya, N. Nishiyama, and S. Arai, "Low-power-consumption high-eye-margin 10-Gb/s operation by GaInAsP/InP distributed reflector lasers with wirelike active regions," IEEE Photonics Technol. Lett. **23**(18), 1349–1351 (2011).

32. W. Hofmann, N. H. Zhu, M. Ortsiefer, G. Bohm, Y. Liu, and M.-C. Amann, "High speed (>11 GHz) modulation of BCB-passivated 1.55 μm InGaAlAs-InP VCSELs," Electron. Lett. **42**(17), 976–977 (2006).

33. M. Muller, C. Grasse, and M. C. Amann, "InP-based 1.3 μm and 1.55 μm short-cavity VCSELs suitable for telecom- and datacom-applications," in *Proc. of 14th International Conference on Transparent Optical Networks* (ICTON, 2012), paper Mo.B4.2.

34. S. Spiga, D. Schoke, A. Andrejew, M. Müller, G. Boehm, and M. C. Amann, "Single-mode 1.5-μm VCSELs with 22-GHz small-signal bandwidth," in *Optical Fiber Communication Conference*, 2016 OSA Technical Digest Series (Optical Society of America, 2016), paper Tu3D.4.

35. H. Nishi, T. Fujii, K. Takeda, K. Hasebe, T. Kakitsuka, T. Tsuchizawa, T. Yamamoto, K. Yamada, and S. Matsuo, "Membrane distributed-reflector laser integrated with SiO_x-based spot-size converter on Si platform," in *Proc. of the 41st European Conference on Optical Communications* (ECOC, 2015), paper We.2.5.3.

1. Introduction

Advances in optical communication technology have enabled high-capacity transmission over a wide range of distances. Short-reach optical communication for board-to-board and chip-to-chip interconnections has been extensively investigated because of the need for high-bandwidth, energy-efficient, and low-cost data transmission [1]. An on-chip optical interconnection is one of solutions for the electrical interconnection problems of large-scale integrated circuit (LSI) [2,3]. Many optical devices have been demonstrated for this purpose. Silicon photonic circuits have demonstrated their advantages of high-index contrast compact optical devices such as external modulators, and photodiodes [4,5], however, they usually use external light source. To integrate lasers on a LSI chip, an ultra-low power consumption semiconductor laser is essential because the energy consumption of the laser should be less than 100 fJ/bit for on-chip interconnection [6]. This energy cost corresponds to the operating conditions of laser bias current of 1 mA by assuming that the data rate and operating voltage are 10 Gbit/s and 1 V, respectively. Several approaches have been demonstrated such as VCSELs [7], microdisc lasers [8], and photonic crystal (PhC) lasers [9]. These lasers demonstrated ultra-low threshold current operation [10,11] and high-speed direct modulation with low energy consumption [11,12]. In addition, to achieve efficient light coupling into an in-plane optical circuit, an easy integration structure with an in-plane waveguide is pertinent.

We have proposed a membrane distributed-feedback laser (DFB) as a light source for on-chip optical interconnects [13,14]. DFB lasers have been widely used as light sources in large-scale photonic integrated circuits [15]. However, typical DFB lasers have threshold current that are in the order of several-mA and require several 10-mA bias current for high-speed direct modulation [16]. These properties result in an energy cost of a few pJ/bit, which is an unacceptably high energy cost for on-chip interconnection. The membrane structure, which consists of a thin semiconductor core layer sandwiched by dielectric cladding layers, was proposed to enhance the optical confinement into the active layer, which result in optical modal gain and high index-coupling coefficient of the DFB grating. These features enable the realization of DFB lasers with low-threshold current operation as well as high-speed direct modulation at low bias current condition, namely high-modulation efficiency. In addition, the membrane structure can be prepared by benzocyclobutene (BCB) bonding on Si substrate at a CMOS-compatible temperature (< 300 °C). Optically pumped membrane DFB lasers have been shown to have low-threshold properties [17–19]. The use of a lateral-current-injection (LCI) structure [20–22] has facilitated the successful operation of injection-type membrane lasers with internal quantum efficiency comparable to that of conventional lasers [23]. Recently, we reported low threshold current [24] and high modulation efficiency operation [25] of membrane DFB lasers. Moreover, integration with a p-i-n photodiode (PD) [26], and a distributed-reflector (DR) laser [27] were realized. Although the low-threshold current and high-speed modulation properties of membrane DFB laser were confirmed, large-signal direct modulation of membrane DFB laser at low-bias current (less than 1 mA) had not yet been demonstrated.

In this paper, high-speed direct modulation of the membrane DFB laser on a Si substrate is reported. A modulation efficiency of 11 GHz/mA$^{1/2}$ was obtained, which enables sufficient bandwidth for 10 Gbit/s direct modulation at a bias current of 1 mA. Large signal direct modulation was performed using a 10 Gbit/s non-return-to-zero (NRZ) 2^{31}-1 pseudo random bit sequence (PRBS) signal. A bit-error rate (BER) of 10^{-9} was obtained with an extinction ratio of 5 dB.

2. Device structure and fabrication

A schematic illustration showing the structure of the fabricated membrane DFB laser is presented in Fig. 1(a). A semiconductor layer with SiO$_2$ cladding was bonded on a Si substrate by using a BCB adhesion layer. The cavity length of the DFB laser was 50 µm. The

DFB laser had a 20-µm-long GaInAsP passive waveguide on the rear side, which was originally prepared to integrate a photodiode. The front side facet was cleaved and the rear side facet was formed by mechanically removing the bonded semiconductor layer. The both facets had no optical coatings. The period of the surface grating formed on the active region was 295 nm. Figure 1(b) shows a cross-section of the active region. The thickness of the semiconductor core layer was 270 nm. The 0.6-µm-wide active layer stripe was placed between the regrown n- and p-InP layers to form an LCI structure. In our previous work, non-alloy Ti/Au was used as a p-side contact electrode, but it resulted in poor electrical resistance. Therefore, alloyed Au/Zn/Au of 25/50/300 nm thickness was introduced as the p-side contact electrode in this work. The main fabrication steps are described in [24]. An initial epitaxial wafer comprises of strain-compensated GaInAsP 5QWs sandwiched by 15-nm-thick GaInAsP optical confinement layers, 50-nm-thick top undoped InP cap, 100-nm-thick bottom p-InP cap ($N_A = 5 \times 10^{17}$ cm^{-3}), and etch stop layers grown on an InP substrate by molecular beam epitaxy. Then, a selective area epitaxial regrowth process using a SiO$_2$ mask was repeated three times to construct a passive GaInAsP waveguide region and a lateral p-i-n diode structure by organo-metallic vapor phase epitaxy. After depositing a SiO$_2$ cladding layer on the InP substrate, the substrate was bonded upside down on a Si wafer and the InP substrate side was removed by polishing and wet chemical etching. Then the Ti/Au n-side and Au/Zn/Au p-side electrodes were formed by electron beam evaporation and thermal evaporation, respectively. Finally, a SiO$_2$ surface grating pattern was defined by an electron beam lithography, then the pattern was transferred onto the surface InP layer by wet chemical etching.
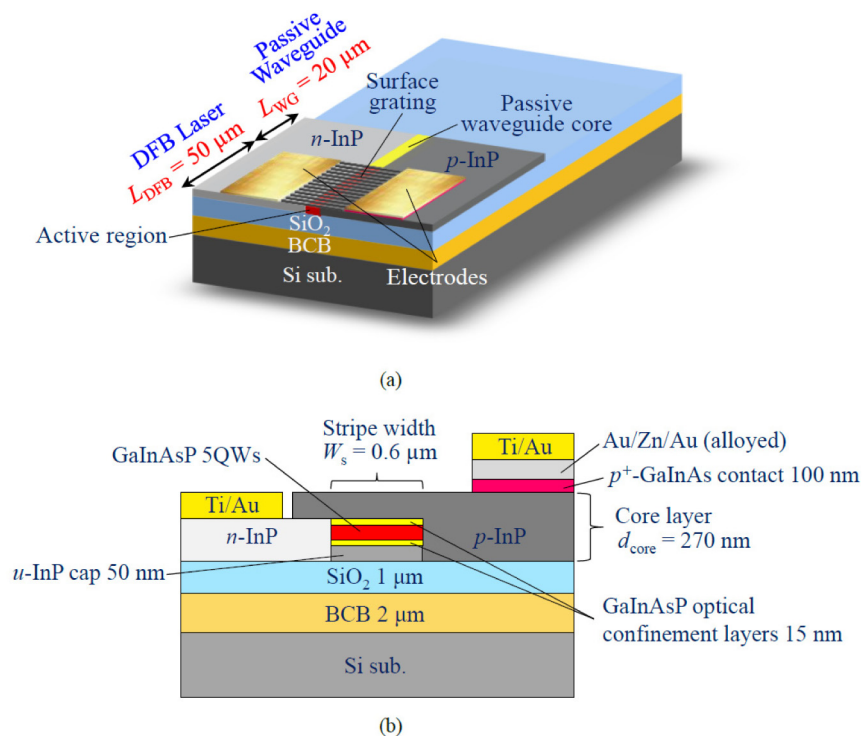

(a)

(b)

Fig. 1. Schematic of the membrane DFB laser structure: (a) top view; (b) cross section of active region.

3. Static characteristics

The static characteristics of the fabricated membrane DFB laser were measured under room-temperature (20 °C) continuous-wave (RT-CW) conditions. Figure 2 shows light output and the voltage versus injection current characteristics. The threshold current I_{th} was 0.21 mA, and the threshold current density was 700 A/cm^2 (corresponding to the threshold current density normalized by the number of quantum-wells of 140 A/cm^2/well.) The external differential quantum efficiency η_d was 5% (front facet). The differential quantum efficiency (5% from the front output) of this device was poorer than that (12% from the front output) reported in [25], but we can't give a clear explanation for this discrepancy because both devices had cleaved facets without anti-reflection coatings. The operating voltage was reduced to approximately half of that previously reported for the same device length [24]; this can be attributed to the introduction of the alloyed Au/Zn/Au electrode. Figure 3 shows lasing spectra measured for different bias currents. Stable single-mode operation was observed for a bias up to 2 mA, after which the light output showed a thermal roll-off. The lasing wavelength was 1542 nm at 1-mA bias current. The sub-mode suppression-ratio (SMSR) was 41 dB and 47 dB at bias currents of 1 mA and 2 mA, respectively. From the lasing spectrum at bias current 2 mA, a stopband width could be determined by measuring the wavelength span where a level of the spontaneous emission intensity was much lower than the noise level of the spectrum analyzer (Ando (currently Yokogawa), AQ6317B). Based on the theory of emission spectrum of the DFB laser [28], the obtained stopband width corresponded to an index-coupling coefficient of 2100 cm^{-1}. The mode span of the spectrum was different from theoretical one. It can be attributed to facet phase of front and rear facets because both facets had no AR coatings.
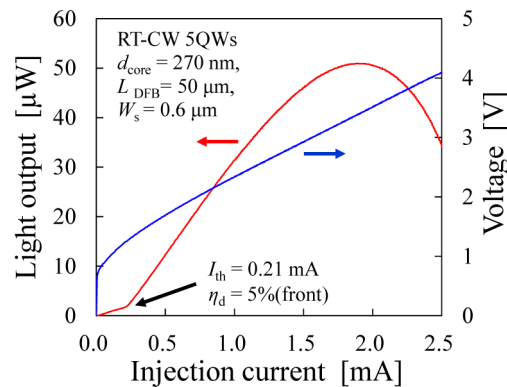

Fig. 2. Light output and voltage versus injection current characteristics of the membrane DFB laser.
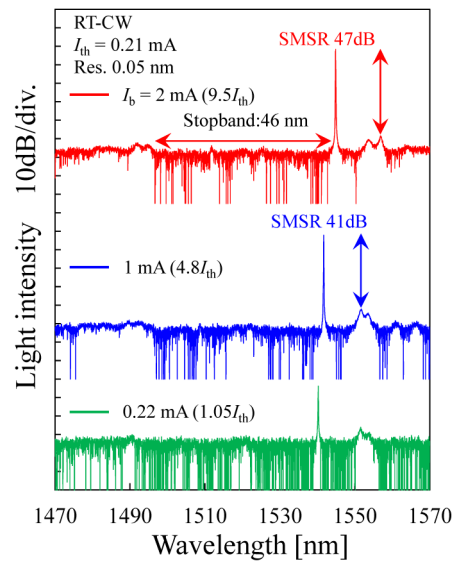
Fig. 3. Lasing spectra measured for three different bias current conditions.

4. Modulation characteristics

The small-signal modulation properties of the membrane DFB laser were measured using a vector network analyzer. A modulation signal was input to the laser using a 40 GHz high-speed ground-signal (GS) RF probe with 100 µm pitch. The light output of the laser was coupled to a spherical-lensed single-mode fiber. A photograph of the device during the measurement is shown in Fig. 4. The collected optical signal output was amplified by an erbium-doped fiber amplifier (EDFA), and then the amplified spontaneous emission (ASE) light was filtered by a tunable bandpass filter. The optical signal was finally detected by a 12 GHz PIN-photoreceiver.

The small-signal responses (S_{21}) of the membrane DFB laser measured at various injection currents from 0.28 to 1.47 mA are shown in Fig. 5(a). Because we obtained 3dB bandwidth of 12.8 GHz at 0.98-mA bias current, 10 Gbit/s operation was considered to be possible with a bias current below 1 mA. The maximum 3-dB bandwidth of 13.6 GHz was obtained at a bias current of 1.47 mA.
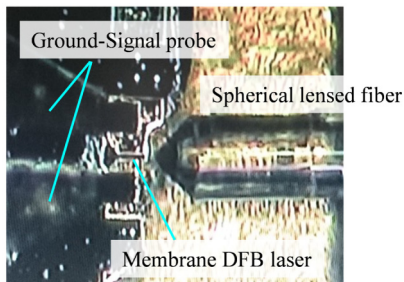

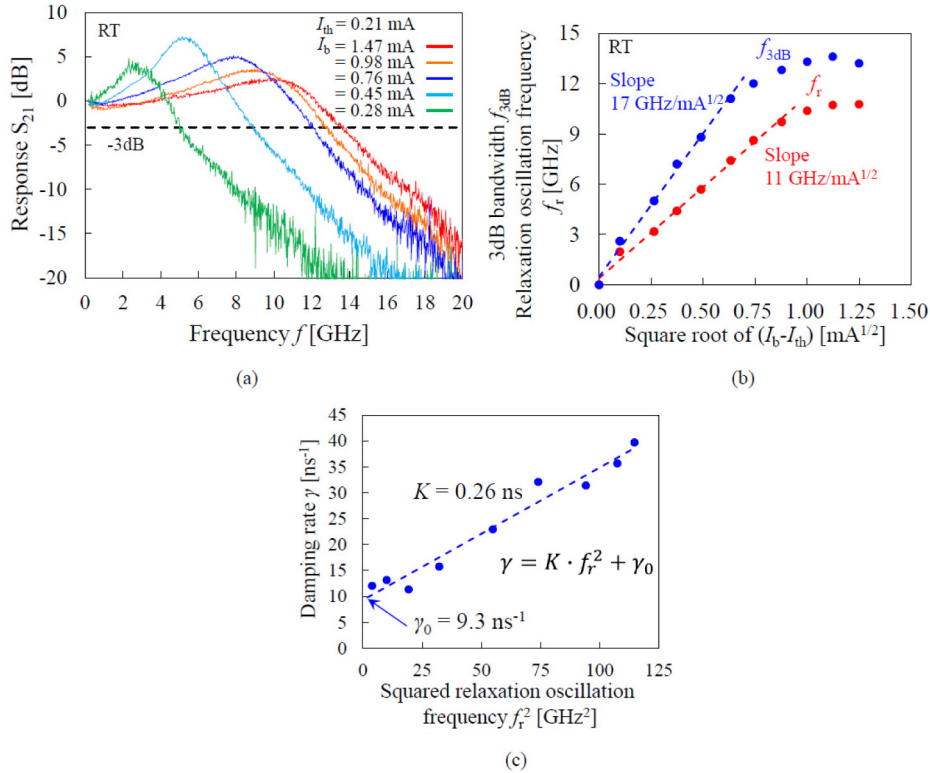Fig. 4. Photograph of the device during modulation measurement.

Fig. 5. Results of small signal modulation measurement, (a) responses of S_{21} measured for various bias current conditions, (b) plots of relaxation oscillation frequency and 3dB bandwidth versus square root of bias current above threshold, and (c) damping factor as a function of the squared relaxation oscillation frequency.

Figure 5(b) shows relaxation oscillation frequency f_r and 3-dB bandwidth f_{3dB} as a function of the square root of bias current above the threshold. The slope efficiencies for f_r and f_{3dB} were 11 GHz/mA$^{1/2}$ and 17 GHz/mA$^{1/2}$, respectively. The damping rate was also extracted from the small-signal responses. Figure 5(c) shows the plots of damping rate versus squared relaxation oscillation frequency. As shown in the inset of Fig. 5(c), the K-factor and intrinsic damping offset γ_0 were obtained from the linear fitting of the plots. The K-factor and offset γ_0 were 0.26 ns and 9.3 ns^{-1}, respectively. The maximum intrinsic bandwidth, $f_{3dB, max}$, is given by [29,30],

$$f_{3dB,\max} = \frac{2\sqrt{2}\pi}{K} \tag{1}$$

The obtained K-factor corresponds to an intrinsic maximum bandwidth, neglecting the self-heating and parasitic cutoff, of 34 GHz. We believe the relaxation oscillation frequency of the current devices shown in Fig. 5(b) was saturated by heating. This can be solved by reducing the electrical resistance as well as thinning BCB layer thickness. Reducing resistance and parasitic capacitance is also important to increase total bandwidth.

The obtained slope efficiency of f_r (modulation efficiency) is compared with that of various lasers, such as InP-based long-wavelength (λ = 1.3–1.55 μm) conventional type DFB lasers, InP-based long wavelength VCSELs and PhC laser as shown in Fig. 6. The conventional DFB lasers demonstrated maximum modulation efficiencies for GaInAsP-based and AlGaInAs-based active layer devices of 3.0 GHz/mA$^{1/2}$ [31] and 4.8 GHz/mA$^{1/2}$ [16], respectively. Great efforts have been paid to enhance modulation efficiency of DFB lasers

mainly by optimizing quantum well structures including well number, width, strain and doping. In contrast, VCSELs demonstrated high modulation efficiency owing to their small-active volume and strong confinement DBRs cavity [32–34]. For membrane DFB lasers, higher efficiencies than conventional DFB lasers have been reported [25,35]. The modulation efficiency of 11 GHz/mA$^{1/2}$ obtained in this work is the highest value reported to date for DFB lasers to the best of our knowledge. This is attributed to the small active volume 50 × 0.6 × 0.03 μm (0.9 μm^3) of the device in this work. We note that a much higher value of 42.4 GHz/mA$^{1/2}$ was reported for a PhC laser using a very small active volume 2.5 × 0.3 × 0.018 μm (0.0135 μm^3, assuming a 6-nm-thick quantum well) [9].
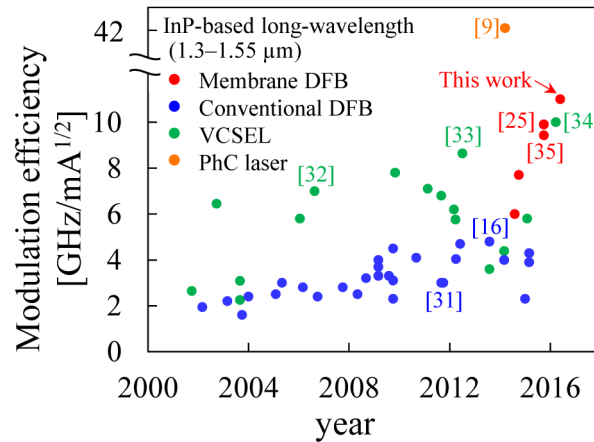

Fig. 6. Recent trend of the modulation efficiency of InP-based long wavelength DFB lasers, VCSELs and PhC laser.

Next, large-signal direct modulation and BER measurements were performed. The optical power was monitored and attenuated by using a variable optical attenuator and power monitor inserted between the output of the bandpass filter and the photoreciever. A modulation electrical signal was generated by a pulse pattern generator. A data signal of non-return-to-zero (NRZ) with a pseudo-random bit sequence (PRBS) having a word length of 2^{31}-1 was used. Figure 7 shows the BER characteristics of the membrane DFB laser at a data rate of 10 Gbit/s as a function of the averaged received optical power. The bias current for the laser and modulation voltage swing were set to 1 mA and 0.52 V$_{pp}$, respectively. We achieved a BER less than 1×10^{-9} at an averaged received power of −5.8 dBm. Figure 8 shows the 10 Gbit/s eye diagram measured under the same modulation conditions. The eye opening was confirmed with an extinction ratio (ER) of 5dB. To the best of our knowledge, this bias current is the lowest value used for 10 Gbit/s large-signal direct modulation of DFB laser, which is attributed to the low-threshold current and high-modulation efficiency characteristics of the membrane DFB structure. Although an error-floor appeared in the BER curve, the linearity of the BER curve and eye opening will be improved if the slope efficiency is improved to the same value as that of a conventional DFB laser.

Then, we calculated the energy cost of these experiments. The driving voltage of the laser was 2.3 V as seen in Fig. 2 at 1-mA bias current. The energy cost per bit for data transmission can be calculated by the product of bias current and voltage divided by the data rate.

$$Energy\ cost = \frac{I_b V_b}{Data\ rate} \qquad (2)$$

According to this relationship, the energy cost was calculated to be 230 fJ/bit. The energy cost achieved was small in comparison to a conventional DFB laser, but it is still approximately twice that achieved by previous research [35]. This is caused by a relatively high driving

voltage because of the differential resistance of 1.2 kΩ. It is expected that the differential resistance can be reduced to 200 Ω by attaining the same electrical characteristics as [35], thereby resulting in a driving voltage of approximately 1 V at 1-mA bias current.
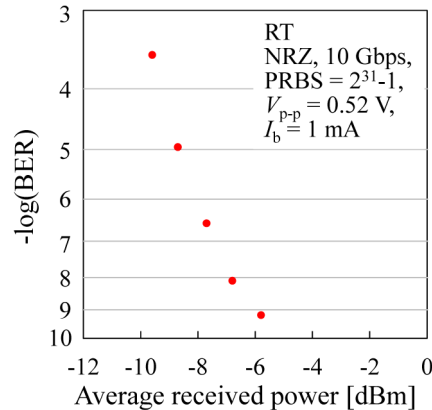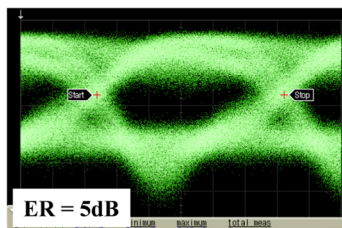

RT
NRZ, 10 Gbps,
PRBS = 2^{31}-1,
V_{p-p} = 0.52 V,
I_b = 1 mA

Fig. 7. 10 Gbit/s BER characteristics.

ER = 5dB

Fig. 8. Eye diagram at 10 Gbit/s of NRZ signal using a 2^{31}-1 pattern.

5. Conclusion

We have demonstrated 10 Gbit/s direct modulation of a membrane DFB laser at 1-mA bias current. The fabricated membrane DFB laser had a threshold current of 0.21 mA, 3dB bandwidth of 12.8 GHz at a bias current of 0.98 mA, and a modulation efficiency of 11 GHz/mA$^{1/2}$. Large-signal direct modulation at 10 Gbit/s was performed using an NRZ signal with PRBS = 2^{31}-1, and we obtained a BER < 1 × 10^{-9}. These results indicate that the membrane DFB laser is a promising light source for ultra-low power consumption operation that is likely to be useful for on-chip optical links.